International Journal of Science and Research (IJSR)
ISSN: 2319-7064
SJIF (2022): 7.942

Analysis of Ocular Coefficients and Ocular Band Gap for Fluid Se40-Xte60agx Tinny Films

Vinyas Goswami[1], Satendra Singh[2]

[1]Research Scholar, Department of Physics, Sunrise University, Alwar, Rajasthan, India

[2]Associate Professor, Department of Physics, Sunrise University, Alwar, Rajasthan, India

Abstract: ***This publication reports the outcome of tableware (Ag) content on the optical package of unmolded chalco-genide plates of Se40-xTe60Agx (x=0, 2, 4, 6, 8). Thin strips of the a-Se40-xTe60Agx glass mixture were produced by using current vaporization under high pressure vacuum conditions (10-5 Torr) using a computer-controlled dual-beam UV-VIS-NIR spectrophotometer in the wavelength range from 200 to 3000 nm. Measured in Calculate the optical constants (refractive index (n), annihilation measurement (k), real permittivity (ε'), imaginary permittivity (ε''), and immersion measurement (α)) using the Goose Paul mode Did. Optical bandgap of unmolded Se40-xTe60Agx flakes. The immersion measurement (α) increases with incident photon energy (hv) for all samples. The optical bandgap increases with increasing dish (Ag) content. The increase in optical bandgap with increasing Ag content was explained based on the Mott and Davis model.***

Keywords: Tinny films, Chalcogenide glasses, Defect states, Optical constants, Optical band gap etc.

1. Introduction

Chalcogenide goggles are oxygen-free inorganic goggles containing one or more chalcogen groups (1-2). These glasses are formed by adding other elements similar to Ag, As, Ge, etc. Chalcogenide glasses are low phonon energy devices and are generally transparent from the visible to the infrared. These glasses are based on sulfides, selenides, and tellurides in binary and multi-element systems, and there is great interest in understanding their mechanisms of action under induced drug and semiconducting biases. These glasses are used in a wide variety of electrical, optical, and optical applications similar to irrecoverable optical phase change recording, memory bias, optical filaments, xerography, photolithography, infrared lenses, optical amplifiers, Blu-ray diodes, and solar cells. It has technical operations (3-12). . Chalcogenide goggles are known to have flexible structures. This means that each snippet can adapt adjacent terrain to meet the Volant's requirements. Chalcogenide goggles are sensitive to the penetration of electromagnetic radiation, display a variety of compelling products, and colorful models have been proposed to illustrate these products, with diffraction, surge, and fiber structures can be used to create (13-14) . Chalcogenide glasses have poor thermomechanical properties, so softening temperature and mechanical strength must be increased to expand the working range. Interest in these finishes arises especially because of their ease of manufacture in the form of large, thin patches. The addition of tellurium (Te) has a catalytic effect on the crystallization of selenium. Since Se–Te bonds are weaker than Se–Se bonds, the presence of Te in the Se chains probably facilitates their thermal dissociation (15). Se–Te mixtures have attracted much attention due to their lower hardness, higher photosensitivity, higher crystallization temperature and lower aging properties compared to pure, unformed Se(16–17). Addition of Se to Te improves corrosion resistance (18). Therefore, the Se-Te ground mixture may be an excellent and promising medium to exploit the phase change between the unformed and liquid states. The effects of contamination on unformed semiconductor materials are highly dependent on the conducting medium and material structure (19). Contamination can destroy pendant binding centers of labels or form charged centers that are compensated by centers of opposite sign. In this study, we chose Ag as the cumulative element in the Se–Te mixture. The third element acts as a chemical modifier as it is said to expand the range of glass formation.

The addition of a third element such as Ag in Se-Te double fusion is expected to modify the optical and electrical package of the host fusion. Typical chalcogenides have fairly sharp optical immersion edges, a single electrical activation energy, effective conductivity, and fluorescence upon compressive motion. Studying the optical package of chalcogenide glasses is important for determining the electronic band structure and other optical parameters as well as the optical energy gap and refractive index. The end of the current work is to study the effect of Ag objectification on the optical packets of Se-Te mixtures. The optical transmittance scale of unshaped a-Se40-xTe60Agx thin films is measured with a spectrophotometer. Optical parameters such as refractive index, extinction exponent, real and imaginary permittivity, immersion index and optical bandgap were calculated for the Se40-xTe60Agx glass system.

2. Experimental Procedure

Glassy mixtures of a-Se40-xTe60Agx (x = 0, 2, 4, 6, 8) were prepared by melt quenching. 99.999 high purity Se, Ag and Te particles were loaded according to the equation a-Se40-xTe60Agx (x = 0, 2, 4, 6, 8). The fat color mixture was placed in a quartz vial and sealed under a vacuum of 10 -5 Torr. The sealed quartz ampoule was loaded into a furnace, heated to 950 °C for 18 h at a rate of 3–4 °C/nsec to ensure compositional homogeneity, and quenched with liquid nitrogen. The beams were squashed, separated, predicted and characterized. The glassy nature of the mixture was confirmed by X-ray diffraction patterns using Cu-Kα

radiation. Chalcogenide flakes were synthesized by thermal evaporation under high vacuum conditions (10-5 Torr) using bulk amalgam flakes as starting material and glass as substrate. The strip was kept in the deposition chamber for 24 hours to achieve metastable equilibrium. Optical transmittance scales of thin strips of unmolded Se40-xTe60Agx (x = 0, 2, 4, 6, 8) were measured at wavelengths using a computer-controlled dual-beam UV-VIS-IR spectrophotometer measured as a function.

3. Result and Discussion

Light transmission (T) is a very complex function, designed to depend on immersionis shown inFig. 1.

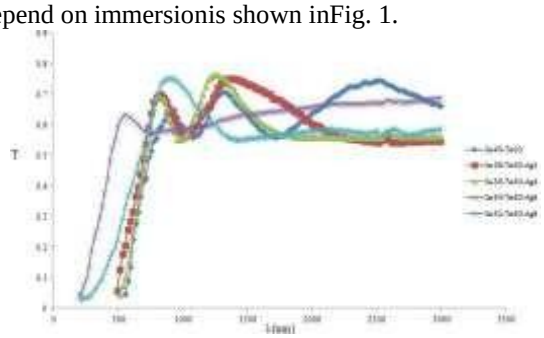

Figure 1: Difference of optical transmittance (T) with wave length (λ) for amorphous $Se_{40-x}Te_{60}Ag_x$ thin films

Through the famous system of Swanepole(20) based on Mainfacer's proposition (21), an envelope of disturbance maxima and minima arises at the diapason, and the presence of this maxima and minima positions gives us: The optical integrity of the deposited film is confirmed, no scattering occurs and no immersion occurs. at long wavelengths. This mode was used by colorful experimenters with chalcogenide glasses (22-23).

Purpose of optical constants

Through Swanepoel's system, in Figure 20, the optical parameters are derived from the boundary pattern of the transmission diapason. In the transmission range where the immersion is (α = 0), the refractive index n is given by

$$n=[N+(N^2-s^2)^{1/2}]^{1/2} \quad (1)$$

Where $N=(2s/T_m)-(s^2+1)/2$, s is the refractive index of the substrate and T_m is the envelope function of the transmittance minima.

Where (α ≠ 0), in the region of weak and medium absorption, the refractive index n is given by

$$n=[N+(N^2-s^2)^{1/2}]^{1/2} \quad (2)$$

Where $N= \{2s(T_M-T_m)/\}T_MT_m+(s^2+1)/2$ and T_m is the envelope function of the transmittance maxima.

In the region of strong immersion, the transmittance decreases drastically and refractive indicator (n) can be estimated by reasoning the values in the other regions. If n1 and n2 are the refractive indicators at two conterminous maxes and minima at λ1 and λ2 also the consistence of the film (d) is given by

$$d = \lambda1\lambda2 / 2[\lambda1n2 - \lambda2n1] \quad (3)$$

The extinction coefficient (k) can be calculated by relation

$$k = \alpha \lambda / (4\pi) = (\lambda / 4\pi d) \ln (1/x) \quad (4)$$

where x is the absorbance and d is the film thickness.

In the region of weak and medium absorption, absorbance (x) can be calculated from the transmission minima Tm and given in equation -5.

$$x = [Em - \{Em - (n2 -1)3 (n2 - s4)1/2] / [(n - 1)3 (n - s2)] \quad (5)$$

Where $Em = [(8n2s/Tm)-(n2-1)(n2-s2)]$

The values obtained for the refractive index and the degree of breakdown are shown in Table 1. Figure 2 shows the change in refractive index with photon energy (hν), and Figure 3 shows the change in annihilation scale with photon energy. 3. Refractive index values and annihilation measures have been observed to show an overall increasing trend with increasing photon energy. From Table 1, it can be seen that the values of refractive index (n) and annihilation (k) increase with increasing Ag content in the a-Se40-xTe60Agx thin films. This spectral and doping dependence of optical constants on photon energy helps determine whether this system is suitable for optical data storage bias operations. The real and imaginary parts of the permittivity of unformed thin strips were independently calculated by relations 6) and (7).

$$\varepsilon' = n2 - k2 \quad (6)$$

$$\varepsilon'' = 2nk \quad (7)$$

Corridors of the real and imaginary permittivity with photon energy are shown in Figures 1 and 2. 4 and 5 are independent. The calculated real and imaginary parts of the permittivity are also shown in Table 1. These are set to increase with increasing photon energy and with the addition of his Ag contamination to the current system of a-Se40-xTe60Agx thin films.

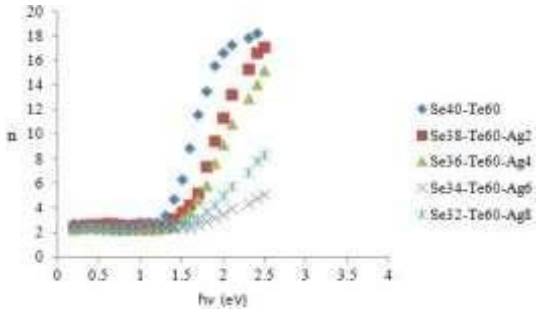

Figure 2: Variation of refractive index (n) with photon energy (hν) for amorphous $Se_{40-x}Te_{60}Ag_x$ thin films

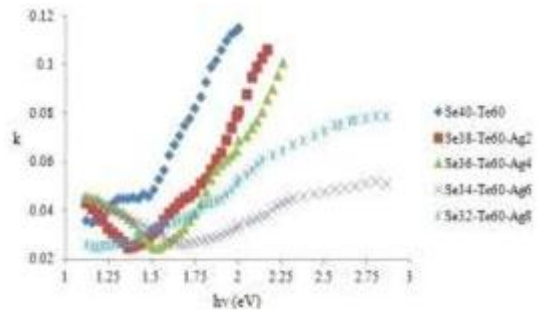

Figure 3: Variation of extinction coefficient (k) with photon energy (hν) for amorphous $Se_{40-x}Te_{60}Ag_x$ thin films

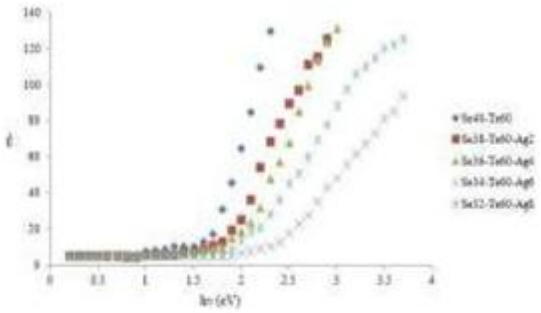

Figure 4: Variation of real dielectric constant (ε') with photon energy (hν) for amorphous $Se_{40-x}Te_{60}Ag_x$ thin films

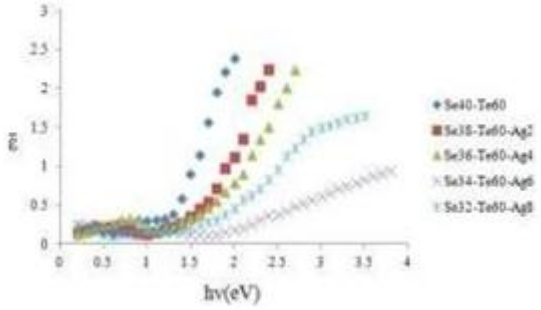

Figure 5: Variation of imaginary dielectric constant with photon energy (hν) for amorphous $Se_{40-x}Te_{60}Ag_x$ thin films

The immersion dimension (α) of the unmolded Se40xTe60Agx thin films was calculated using the relationship (8).

$$\alpha = 4\pi k / \lambda \quad (8)$$

Next, we also observe an increase in the value of immersion (α) with increasing photon energy in the a-Se40-Te60Agx flakes, and an increase in the value of immersion with increasing Ag content. Due to their high degree of immersion, these devices are suitable for biasing optical memories.

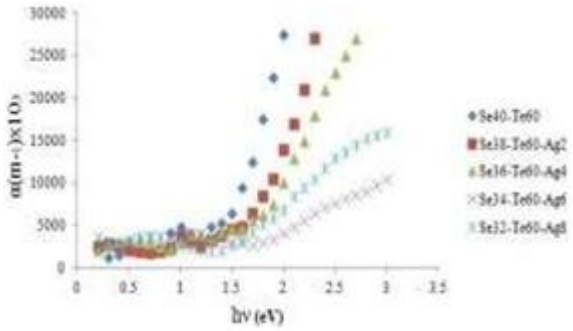

Figure 6: Variation of absorption coefficient (α) with photon energy (hν) for amorphous $Se_{40-x}Te_{60}Ag_x$ thin films

The optical bandgap is calculated from the immersion measurement data as a function of energy (hν) using the Tauc relation (24-25).

$$\alpha = A(h\nu - E_g)^n / h\nu \quad (9)$$

Then A is a constant. For example, the material's optical bandgap and exponent n depend on the type of transition, with values 1/2, 2, 3/2, and 3 corresponding to allowed direct, allowed cyclic, and forbidden direct. hold. Independently of each other, they correspond to forbidden cyclic transitions. The current system of a-Se40-xTe60Agx follows the allowed circular transition rule.

Optical bandgap (Eg) values are calculated by establishing the linear segment of (αhν) 1/nvs. Calculate hν for n = 2 as shown. 7. The calculated values of Eg for all samples are shown in Table 1. From Table 1, we can see that the optical bandgap (Eg) increases with increasing Ag content. The increase in optical bandgap with increasing Ag content can be explained based on the model by Mott and Davis (24). According to this epidemic, strain states are of great interest in chalcogenide thin films, and these corruptions are responsible for the presence of localized states within the bandgap. Fig. 1 shows the change in the optical bandgap due to dish attention. 8.The increase in optical bandgap with increasing Ag content may be due to a decrease in viscosity or an increase in disorder in the strain state of the mobility gap. The increase in optical bandgap with decreasing viscosity of the deformed land can also be discerned by the electronegativities of the primordial groups involved. The electronegativities of Se, Te, and Ag are 2.4, 2.1, and 1.93, respectively, with Ag being less electronegative than Se. The flounce bands of the chalcogenide glasses contain the p-orbitals of the credit bracket, and adding an electropositive element (Ag) to the electronegative element (Se) increases the energy of the credit bracket country, which is the extent of the credit bracket Further explain the expansion of its flounces the band within the forbidden bandgap, leading to band trailing and widening of the bandgap.

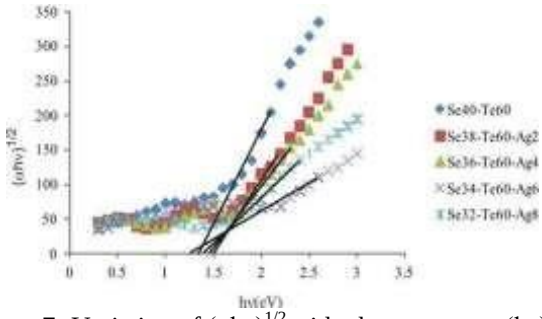

Figure 7: Variation of $(\alpha h\nu)^{1/2}$ with photon energy (hν) for amorphous $Se_{40-x}Te_{60}Ag_x$ thin films

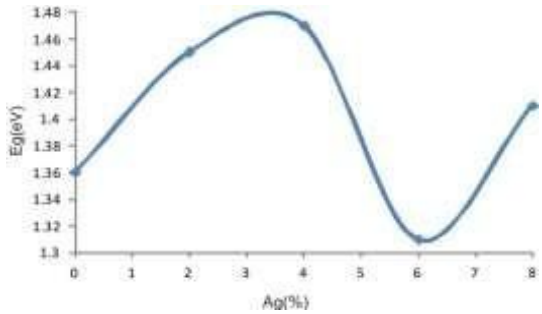

Figure 8: Variation of optical band gab (Eg) with silver (Ag) concentration for amorphous Se40- xTe60Agx thin films

Table 1: Optical parameters for amorphous Se40-xTe60Agx thin films at 1600 nm

Material	Refractive Index (n)	Extinction Coefficient (k)	Real Dielectric Constant (ε′)	Imaginary Dielectric Constants (ε″)	Absorption Coefficient (α)(m^{-1}) x 10^3	Optical Band Gap Eg (eV)
$Se_{40}Te_{60}$	16.65	0.115	65.00	2.39	27.50	1.36
$Se_{38}Te_{60}Ag_2$	11.35	0.081	25.25	1.12	14.00	1.45
$Se_{36}Te_{60}Ag_4$	9.15	0.069	19.33	0.79	10.10	1.47
$Se_{34}Te_{60}Ag_6$	3.55	0.034	7.23	0.18	4.10	1.31
$Se_{32}Te_{60}Ag_8$	5.05	0.053	14.15	0.46	6.90	1.41

These circular bandgap instruments can operate implicitly in optical recording media, infrared spectroscopy, filament emission, xerography, fiber optic communications, and electrophotographic manipulation. Refractive index and translucency in the infrared are also good indicators for integrated optics and discoveries in the near-infrared spectral range.

4. Conclusions

Thin films of a-Se40-xTe60Agx glassy mixture were synthesized by thermal evaporation under high vacuum conditions (10-5 Torr) using unshaped bulk amalgam as starting material and glass as substrate. . x = 0, 2, 4, 6, 8) thin strips were measured with a computer-controlled UV-VIS-NIR double-beam spectrophotometer. The Swanepole system was used to calculate refractive indices, real and imaginary permittivity, annihilation measurements, immersion measurements, and optical band gaps. Refractive index (n), annihilation measurements (k), real permittivity (ε′), imaginary permittivity (ε′), and immersion measurements (α) increase with increasing photon energy, increasing attention of Ag up to x = 0.2. decreases with Change 4 and 6 and increase all calculated optical parameters of Ag at x=8. The optical band gap (Eg) increases with increasing Ag content. The increase in optical bandgap with increasing Ag content may be due to the decrease in viscosity of the deforming state within the mobility gap. Alternatively, increased disorder and post-order may be possible for x = 8 specific attention in the study sample. However, at x = 6 for Ag content, the minima of the optical bandgap and other optical parameters, thereby increasing the viscosity of the warped state or reducing the mobility gap hindrance due to this attention of Ag Based on the optical parameter values calculated above, the suitability of these optical bearing bias devices can be determined.

References

[1] J. S. Sanghera, J. Heo, J. D. Mackenize, J. Non-Cryst. Solids **103**,155(1988).
[2] V. Pandey, S. K. Tripathi, A. Kumar, Journal of Ovonic Research **2**, 67(2006).
[3] M. Saxena, S. Gupta, A. Agarwal, Adv. Appl. Sci. Research **2** (2), 109(2011).
[4] G. Kaur, T. Komatsu, J. Mater. Sci.**36**, 453(2001).
[5] Z.Abdel- KhalekAli, G. H. Adel, A. S. Abd-rbo, Chalc. Lett. **6**,125(2009).
[6] V. Trnovcona, I.Furar, D. lezal, J. Non-Cryst.Solids **353**, 1311(2007).
[7] A.Kumar, P. B.Barman, R. Sharma, Adv. Appl. Sci. Research **1**(2), 47(2010).
[8] A.Kumar, M. Lal, K. Sharma, S. K. Tripathi, N.Goyal, Chalc. Lett.**9**, 275(2012).
[9] V. K. Saraswat, V. Kishore, K. Singh, N. S. Sexana, T. P. Sharma,Chalc. Lett.**3**,61(2006).
[10] R. M. Mehra, G. Kaur, P. C. Mathur, J. Mater.Sci. **26**, 3433(1991).
[11] A. A. Manshina, A. V. Kurochkin, S. V. Degtyarev, Ya. G. Grigoriev, A. S. Tverjanovich, Yu. S. Tveryanovich, V. B. Smirnov, Proc. SPIE**4429**, 80(2001).
[12] A.S.Tverjanovich, Ya. G. Grigoriev, S. V. Degtyarev, A. V. Kurochkin, A. A. Manshina, Yu. S. Tveryanovich, J. Non-Cryst.Solids **286**, 89 (2001).
[13] A. B. Seddon, J. Non-cryst. Solids **44**,184(1995).
[14] J. S. Sanghera, I. D. Agrwal, J. Non-cryst. Solids **6**, 256 (1999).
[15] M.Saxena, J. PhysicsD: AppliedPhysics**38**,460(2005).
[16] R. K. Shukla, S. Swaroup, A. Kumar, A. N. Nigam, Phys. Stat. Sol. (a)K**105**,115(1989).
[17] H. Yang, W. Wang, S. Min, J. Non-cryst. Solids **80**, 503 (1986).
[18] R.Chiba,N.Funakoshi,J.Non-cryst. Solids **105**, 149 (1988).
[19] N.F.Mott, Philos.Mag.**19**,835 (1969).
[20] R. Swanepoel, J. Phys. E.16, (1983)1214.
[21] J. C. Manifacier, J. Gasiot, J. P. Fillard, J. Phys. E. Sci.Instrum.**9**, 1002(1976).
[22] S. M. Ei-Sayed, Vaccum **72**,169(2004).
[23] H. S. Metcoally, Vaccum **62**,345 (2001).
[24] N.F.Mott, E. A. Davis, Electronic Processesin Non-Crystalline Mat., Clarendon, Oxford, 1979, 428.
[25] M. M. Wakkad, E. Kh. Shoker, S. H. Mohamed, J. Non- Cryst.Solids **157**, 265(2000).